

## Toward a novel high-resolution modeling approach for the study of chemical evolution of pollutant plumes during long-range transport

E. Real,<sup>1,2</sup> I. Pisso,<sup>1,3</sup> K. S. Law,<sup>1</sup> B. Legras,<sup>4</sup> N. Bousserrez,<sup>5,6</sup> H. Schlager,<sup>7</sup> A. Roiger,<sup>7</sup> and J. L. Attié<sup>5</sup>

Received 8 January 2009; revised 8 January 2010; accepted 16 February 2010; published 18 June 2010.

[1] This paper presents results from a new method, ZooM-CiTTY, that aims to accurately reproduce filamentation observed in profiles of chemically active species in the free troposphere. Lagrangian tracer reconstructions of aircraft measurements across pollutant plumes including a stochastic representation of mixing are coupled with photochemical trajectory simulations, initialized with global model fields. The results provide a high-resolution simulation of trace gases along the flight track together with a detailed picture about the multiple air mass origins influencing chemical composition in the region where plume measurements were taken. This paper builds on results from Pisso et al. (2009) for the dynamic part of the model (the stochastic tracer reconstructions) and focuses on reconstruction of reactive species like O<sub>3</sub>. The model is evaluated for a case of long-range transport of a forest fire plume from Alaska to Europe. Simulated trace species are compared with measurements made in the plume by the DLR Falcon aircraft flying over Europe, and the role of photochemistry in governing the chemical composition across the plume is evaluated. It is shown that the model reproduces well O<sub>3</sub> and NO<sub>y</sub> concentrations and O<sub>3</sub> production per CO in the plumes as well as gradients at plume edges. In particular, because ZooM-CiTTY represents the contribution of several air masses to a measurement at a particular location, the model can reproduce so-called mixing lines between air masses. Results show that photochemistry and mixing contributions vary in different parts of the plume and that resulting trace gas correlations are a combination of these different mixtures. One limitation of the method is the fact that mixing between air masses is only performed at the end of the trajectories. Errors on simulated O<sub>3</sub> reconstruction from this formulation are evaluated. These errors seem to be negligible in this case (in the free troposphere, far from emission region) because strong gradients are maintained by large-scale winds. Results from ZooM-CiTTY are also used to evaluate errors due to nonlinearities in O<sub>3</sub> photochemistry in coarse-grid models. It is shown that in cases where strong gradients are maintained, errors in net O<sub>3</sub> production can be as high as 50% at plume edges. This new method is interesting to simulate relatively small layering structures observed in the free troposphere, but a more realistic treatment of mixing “en route” is needed if the model has to be used more extensively.

**Citation:** Real, E., I. Pisso, K. S. Law, B. Legras, N. Bousserrez, H. Schlager, A. Roiger, and J. L. Attié (2010), Toward a novel high-resolution modeling approach for the study of chemical evolution of pollutant plumes during long-range transport, *J. Geophys. Res.*, 115, D12302, doi:10.1029/2009JD011707.

### 1. Introduction

[2] Long-range transport of pollutants can impact background levels of pollutants downwind from source regions as well as climate change through perturbations in concentration

distributions. Quantification of long-range transport of pollutants requires the use of numerical models including treatments of emissions, transport (advection, convection, etc.), photochemical and/or aerosol processes, and loss processes such as wet and dry deposition. Evaluation of such numerical

<sup>1</sup>Université Pierre et Marie Curie, Université Versailles-St-Quentin, CNRS, INSU, LATMOS, IPSL, Paris, France.

<sup>2</sup>Now at CEREA, ENPC, EDF, Université Paris-Est, Mame le Vallée, France.

<sup>3</sup>Now at DAMTP, University of Cambridge, Cambridge, UK.

<sup>4</sup>Laboratoire de Météorologie Dynamique, IPSL, Paris, France.

<sup>5</sup>Laboratoire d'Aérodynamique, CNRM, Toulouse, France.

<sup>6</sup>Now at Department of Physics and Atmospheric Science, Dalhousie University, Halifax, Nova Scotia, Canada.

<sup>7</sup>Deutsches Zentrum für Luft- und Raumfahrt, Institut für Physik der Atmosphäre, Wessling, Germany.

models against observations often forms a key part of such studies. Since long-range transport occurs over intercontinental scales, global models are the usual tools applied to quantify its impact. However, given their global nature, these models are often run with horizontal resolutions around  $1^\circ$  to  $2^\circ$  (100 to 200 km). This means that air masses which are as much as 200 km apart are mixed and chemical reactions between these air masses are simulated. This leads to a non-realistic uniformity of trace species and their chemical products like  $O_3$  [Pyle and Zavody, 1990; Crowther et al., 2002; Wild and Prather, 2006] or OH [Esler et al., 2001, 2004] that are dependent on precursor concentrations in a nonlinear manner. These biases can be important close to emission regions [Jacob et al., 1993] because global models do not capture strong local gradients. They may also be important in the free troposphere in regions where local dynamic barriers exist that separate air masses with different chemical composition, such as in the tropopause region [Esler et al., 2001], or in the vicinity of frontal zones [Esler et al., 2003]. Strong gradients can also exist between pollution plumes transported over long distances and background concentrations. As well as errors in chemical rate calculations, errors can also arise due to the use of average winds on the model grid and the calculation of advective transport of trace species [Rolph and Draxler, 1990]. Since global models are unable to reproduce small-scale features, comparisons between measurements and model concentrations requires the degradation of the measurement resolution toward the coarse global model resolution, which implies a loss of information. The use of high-resolution models will be the solution. However, global models are currently limited to 100 km sometimes with a zoom over a particular region down to 50 km. Mesoscale models are run at higher horizontal resolutions (few kilometers to  $0.5^\circ$ ) but are limited in their spatial domain and unable to simulate intercontinental transport, at the present time.

[3] Among the models and methods that have been developed to simulate atmospheric processes Lagrangian deterministic reconstructions or reverse domain filling (RDF) techniques are able to reproduce large observed concentration variability and layering produced by long-range transport [e.g., Methven et al., 2003]. They are based on the principle that atmospheric flows are stratified, and that the majority of phenomena creating filamentation are resolved by large-scale meteorological winds. Although several studies have shown the validity of such an approach for tracers, they underline its tendency to reproduce more variability and fine-scale structure than observed [Methven and Hoskins, 1999] because they lack small-scale turbulence which smears out gradients.

[4] This effect is visible for all trace species but may be more evident in the reconstruction of chemically reactive species such as  $O_3$ , where concentrations in an isolated parcel can be enhanced or reduced by photochemical or physical processes. Indeed, whereas air masses are artificially mixed in a chemical transport model (CTM), they are artificially unmixed in a classical Lagrangian reconstruction model.

[5] In order to introduce turbulent diffusion in Lagrangian calculations, Legras et al. [2003] developed an original method for the stratosphere in which Lagrangian reconstructions include a stochastic mixing process. In a companion paper to this article, Pisso et al. [2009] applied this stochastic Lagrangian reconstruction method to the reconstruction of CO profiles measured by aircraft in the free

troposphere. They focused on reconstruction of air masses originating from Alaskan Forest Fire (FF) emissions with high CO concentrations sampled over the North Atlantic and over Europe during the International Consortium for Atmospheric Research on Transport and Transformation (ICARTT) campaign in July 2004. They showed that this method is able to simulate observed variability of plume CO in the free troposphere and estimated turbulent diffusivity coefficients for this region at this time of the year. They also estimated that in order to reproduce observed features, and by implication, long-range transport of such plumes, global models need to be run at at least 40 km in the horizontal and 500 m in the vertical. The case studied by Pisso et al. [2009] was already examined in detail by Real et al. [2007]. A photochemical trajectory model was initialized with upwind observations and compared to downwind observations in order to evaluate the relative roles of photochemistry and mixing during long-range transport inside this plume.

[6] Here, we take a different approach and couple the high-resolution reconstructions of Pisso et al. [2009] to the same photochemical trajectory model used by Real et al. [2007] to create a first version of a new hybrid model ZooM-CiTTY (Zoom Model for Chemical Transformations and Transport). The aim of this work is to reproduce measured aircraft observations of chemically active species such as  $O_3$  using this new approach which can take into account the multiple origins of air masses influencing individual measurements taken across a plume as well as their chemical evolution. This method also allows the evaluation of dynamical and chemical processes acting on different parts of the plume and their relative contributions to observed trace gas correlations and the formation of mixing lines. We use as well ZooM-CiTTY results to examine possible errors in net photochemical production related to resolution and provide an estimate of the horizontal resolutions required in global models to simulate the long-range transport of chemically active species.

[7] A description of the models and data used is given in section 2. This is followed by model validation (see section 3) focusing on the model to data comparison as well as comparison with work by Real et al. [2007]. An evaluation of errors due to the mixing procedure in ZooM-CiTTY is discussed in section 4 and an estimation of errors in coarse grid global models due to nonlinearities in photochemistry using results from ZooM-CiTTY is presented in section 5. Finally conclusions are presented in section 6.

## 2. Data, Methods, and Models

### 2.1. ITOP/ICARTT Campaign

[8] All measurements used in this paper were taken during the ICARTT campaign [Fehsenfeld et al., 2006] which took place in summer 2004 over the North Atlantic. One objective of this campaign was to perform a Lagrangian study of polluted air masses transported across the North Atlantic. One interesting feature was the transport in the free troposphere of FF plumes from Alaska over the North Atlantic to Europe. In particular, as part of the Lagrangian experiment, one of these plumes was sampled several times during its transport over the North Atlantic. Methven et al. [2006] showed that this plume was first intercepted on 18 July over Newfoundland by the NASA-DC8 aircraft, then 2 days later by the UK BAe-146 aircraft over the Azores, and finally on 23 July by the DLR

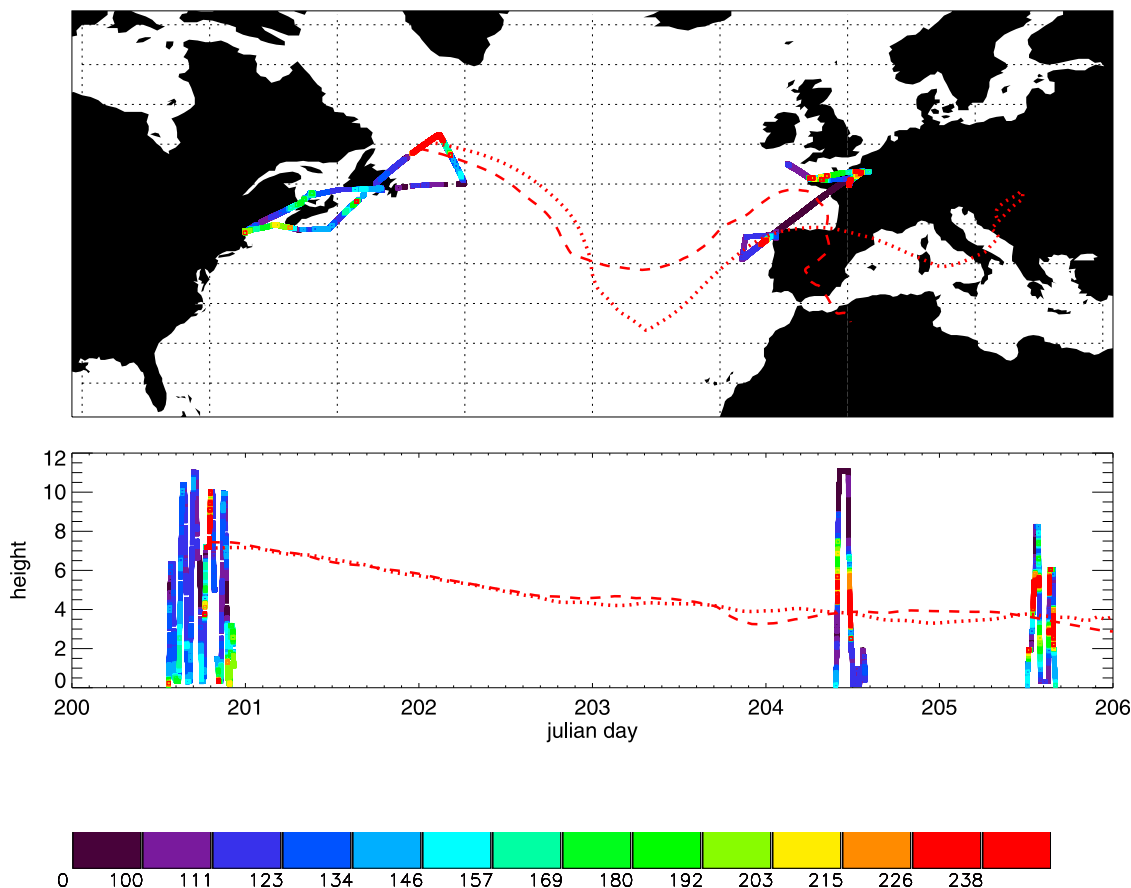


**Figure 1.** (top) DC8 (on 18 July) and Falcon (on 22 and 23 July) flight tracks colored with measured CO (in ppbv). Two forward trajectories from the DC8 aircraft are also represented as red lines. (bottom) Altitude of the aircraft and trajectories with time.

Falcon aircraft over northern France. *Real et al.* [2007] also showed that the same plume was intercepted by the DLR Falcon on 22 July off the coast of Spain. Over the North Atlantic, the FF plume showed very high CO concentrations (averaging around 440 ppbv), high PAN concentrations and moderate levels of O<sub>3</sub> (around 60 ppbv). When intercepted over Europe 5 days later, CO concentrations had decreased to around 250 ppbv but O<sub>3</sub> levels increased by almost 17 ppbv (see DC8 and Falcon flight tracks on Figure 1). *Real et al.* [2007] analyzed the processes leading to this observed chemical evolution using a photochemical model initialized with upwind measurements (over North America) to reproduce observed concentrations downwind (over Europe). Mixing was constrained by observed CO decreases. They showed that the O<sub>3</sub> increase is mainly due to PAN decomposition during plume subsidence, and that mixing with background air masses was also an important factor.

## 2.2. Methodology

[9] The chemical reconstructions performed in this paper are based on the method developed by *Legras et al.* [2003]. This involves calculation of multiple ensembles of trajectories or parcels which arrive at each measurement point along a flight track. Parcels are initialized with CO concentrations from global model fields several days earlier. Stochastic perturbations to parcel positions in the vertical or horizontal

allows the determination of an average turbulent diffusivity,  $D_z$ , acting on all parcels. Agreement between measurements along the flight track and average concentrations calculated using parcel ensembles at each point provides the best estimate of  $D_z$  for different plume samplings. The method relies on the assumption of strong vertical stratification in the atmosphere and requires a large number of particles per individual measurement point. For example, *Pisso et al.* [2009] used 500 or 1000 parcels every 15s or 30s along the flight tracks to reconstruct observed CO.

[10] Here, the multiple ensembles of trajectories used to reconstruct CO by *Pisso et al.* [2009] were coupled with chemical simulations using a Lagrangian photochemistry model (CiTTyCAT, see section 2.3) in order to reconstruct observations of reactive species like O<sub>3</sub> or NO<sub>y</sub>. For each parcel, the chemical model was initialized with global model concentrations at the initial parcel position and time, and its chemical evolution was simulated along the trajectory, forward in time. Therefore, for each measurement point, N chemical simulations were performed along N trajectories. Finally, the N simulated concentrations of each species were averaged at the end point and compared to the measurements along the flight tracks. This method leads to very high resolution simulations (500 (100) particles released every 30 (15) s represent approximately a resolution of 1 (2.5) km) of chemically active species from low-resolution model fields,

which can be directly compared to measurements in a particular plume. Since it allows a magnification in terms of resolution compared to the original global model we call this coupled model ZooM-CiTTY.

[11] As mentioned earlier, mixing is simulated by applying a turbulent diffusivity to parcel positions along the N trajectories. During their transport the parcels are isolated from each other and only mixed at the end points which may lead to unrealistic concentrations in some cases. The errors due to this assumption are examined in section 4.

### 2.3. Chemical Models

[12] ZooM-CiTTY is based on combining 2 models: a dynamic one, described by *Pisso et al.* [2009] and a chemical one (CiTTYCAT). Concentration fields from a global model are needed to initialize concentrations of all chemical species. Here we use results from MOCAGE (MODèle de Chimie Atmosphérique à Grande Echelle, Model of Atmospheric Chemistry at Large Scale) model.

#### 2.3.1. CiTTYCAT

[13] The Lagrangian photochemical model CiTTYCAT (Cambridge Tropospheric Trajectory model of Chemistry And Transport) has been used to examine the origin of polluted layers over the North Atlantic during previous aircraft campaigns [*Wild et al.*, 1996; *Evans et al.*, 2000]. This model also successfully captured the evolution of O<sub>3</sub>, CO and other trace species in the Lagrangian FF plume case considered here [*Real et al.*, 2007]. Ninety chemical species are used in the model including degradation of 14 hydrocarbons using chemical rate data from JPL (2003), and updates discussed by *Arnold et al.* [2007]. The photolysis scheme used in the model is based on a two-stream scattering scheme [*Hough*, 1988].

#### 2.3.2. MOCAGE

[14] Global fields from the MOCAGE CTM with a  $2 \times 2$  degree horizontal resolution were used to initialize the multiple trajectory calculations both in this study and the CO fields used by *Pisso et al.* [2009]. MOCAGE uses a semi-Lagrangian advection scheme, and was run with a vertical resolution along its 47 hybrid ( $\sigma - p$ ) levels from 40 to 400 m in the lower troposphere to about 800 m in the tropopause region. The chemical scheme combines the stratospheric REPROBUS [*Lefevre et al.*, 1994] and the tropospheric RACM [*Stockwell et al.*, 1997] schemes. The model was run for the period from June to August 2004 forced with meteorological analyses from Meteo France. Daily FF emissions (CO, NO, VOC) for Canadian/Alaskan regions were used [*Pfister et al.*, 2006]. A detailed evaluation of the model against observations during ICARTT is given by *Bousserez et al.* [2007]. A zoom version of the model with a  $0.5 \times 0.5$  degree horizontal resolution over the North Atlantic was also performed to compare results from ZooM-CiTTY to higher resolution results from an Eulerian model.

### 2.4. Chemical Initialization

[15] Chemical initialization has a very important impact on final ZooM-CiTTY results. It is important that the global model correctly reproduces the main atmospheric features during the period of initialization. *Pisso et al.* [2009] used MOCAGE CO concentrations to initialize back trajectories on 15 July (day of the FF plume emissions) to produce reconstructions for 18, 22 and 23 July which agree well with the CO aircraft measurements after applying different values

of  $D_z$ . These results imply that MOCAGE simulated the location of FF plumes over emission regions on the 15 July at the right place and with correct CO values. *Bousserez et al.* [2007] also showed that the model correctly reproduced observed CO from MOPITT over the North Atlantic during this period.

[16] However, when MOCAGE concentrations are used in ZooM-CiTTY, chemically active species like PAN or O<sub>3</sub> agree less with measurements inside FF plumes downwind. For example, the CO peak measured on 18 July is well represented by MOCAGE [see *Pisso et al.*, 2009, Figure 1] but O<sub>3</sub> is overestimated by more than 40 ppbv (not shown). This overestimation of O<sub>3</sub> production downwind from the FF emission region is not a result specific to MOCAGE, and was also found by *Cook et al.* [2007] and by I. Bey (personal communication, 2009) using different models (TOMCAT and GEOS-CHEM) as well as different daily FF emissions [*Turquety et al.*, 2007; *Pfister et al.*, 2006]. The reason for this overestimation is not clearly understood. It may be due to the incorrect simulation of FF injection heights in global models (leading to too much PAN decomposition), inhibition of O<sub>3</sub> photochemical production by aerosol [*Real et al.*, 2007] or unrealistic emission ratios (NO<sub>x</sub>/CO) [*Cook et al.*, 2007; *Bousserez et al.*, 2007]. Outside FF plumes, the MOCAGE model performs reasonably well even if it has a tendency to overestimate PAN and O<sub>3</sub> concentrations in the lower troposphere [*Bousserez et al.*, 2007].

[17] Since a goal of this paper is to show the ability of the ZooM-CiTTY model to simulate observed fine-scale chemical features starting from coarse global chemical fields, more realistic initial pollutant concentrations are required. Previous studies showed a clear link between measurements in the FF plume on 22 and 23 July and 18 July. Therefore, it was decided to reconstruct the measurements taken on 22 and 23 July using initial concentration field on 18 July. These initial MOCAGE fields were forced toward measured values of O<sub>3</sub> and precursors taken in the FF plume on 18 July. MOCAGE concentrations outside the FF plume were not changed. In practice, linear correlations  $X_{meas}/CO_{meas}$  between CO and other species X (O<sub>3</sub>, NO<sub>y</sub> and VOC) measured by the DC8 in the FF plume on 18 July were established. CO and acetylene concentrations simulated by MOCAGE were used to determine the localization of FF plumes in the global model: an air mass having CO and C<sub>2</sub>H<sub>2</sub> concentrations above 120 ppbv and 1000 pptv, respectively, was considered to be an FF air mass. Indeed, in FF plumes MOCAGE simulated high CO values but also high C<sub>2</sub>H<sub>2</sub> values in contrast to anthropogenic plumes (lower C<sub>2</sub>H<sub>2</sub>). Finally, for air masses considered as FF, MOCAGE concentrations  $X_{sim}$  (O<sub>3</sub>, NO<sub>y</sub> and VOC) were replaced by:  $X_{meas}/CO_{meas} \times CO_{sim}$ . Using this scaling method assured more accurate values of initial concentrations for O<sub>3</sub> and its precursors per simulated CO in the plume.

## 3. Model to Data Comparison

[18] In the ZooM-CiTTY runs only the Lagrangian match samplings of the FF plume were reconstructed on 22 and 23 July. On 23 July ensembles of 500 back trajectories (N = 500) were released every 30 s and on 22 July ensembles of 100 back trajectories (N = 100) were released every 15 s. On the 22 July, the higher temporal resolution compensates the smaller number of particles. Adding parcels or back trajec-

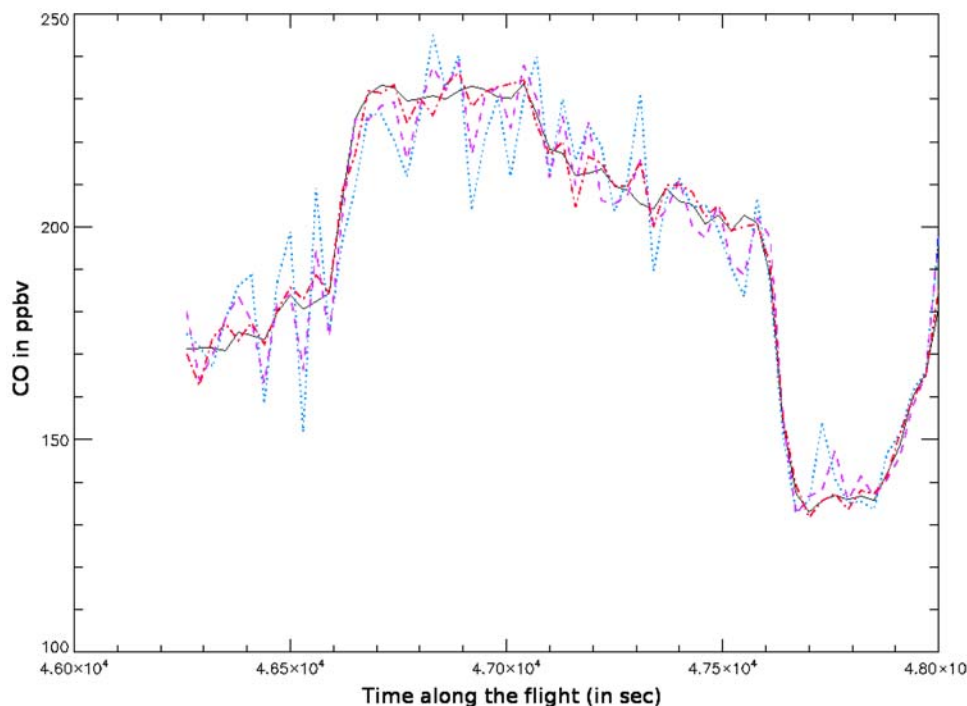


**Figure 2.** ZooM-CiTTY reconstructed CO (in ppbv) for the first part of the Flacon 23 July 2004 flight with 50 (blue dotted line), 100 (violet dashed line), 500 (red dash-dotted line), and 2000 (black solid line) particles initialized every 30 s along the flight track.

ories (increasing  $N$ ) does not produce more realistic spatial variability. This is illustrated in Figure 2 which shows CO reconstructions using 50, 100, 500 and 2000 parcels for the 23 July plume sampling. Reconstructions with 500 and 2000 parcels are not very different compared to reconstructions with value of  $N$  below 500.

### 3.1. The 23 July DLR Falcon Flight Reconstruction

[19] ZooM-CiTTY was applied to the part of 23 July flight highlighted in yellow in Figure 3. This corresponds to the FF plume already sampled by the DC8 on the 18 July. The ZooM-CiTTY reconstructions provide information about the influence of multiple air mass origins and their chemical evolution on downwind concentrations measured by the Falcon both inside the plume and at its edges. Whereas pollutant concentrations can be compared with the observations, net  $O_3$  production in the plume can be compared with those calculated by Real *et al.* [2007]. In that latter study, the simulations were initialized with observations (mean concentrations  $\pm$  standard deviation) taken upwind in the Lagrangian match on 18 July. Mixing was simply parametrized, considering that mean concentrations of the plume decreased uniformly toward background concentrations in an exponential way (based on CO decreases). This parametrization assumed mixing in a plume is uniform, which means that every part of the plume is mixed with the same background air at the same rate.

#### 3.1.1. Time Series Comparison

[20] Observed and simulated CO from MOCAGE (interpolated along the flight track) with a  $2 \times 2$  and a  $0.5 \times 0.5$  degree resolution on 23 July are shown in Figure 3. (In

Figures 1–13, measurements are 1 s averaged.) As already noted by Pissu *et al.* [2009], MOCAGE results interpolated along the flight track are smeared out and the first observed CO peak from FF have almost disappeared with both resolution. The second peak is better represented with the 0.5 degree resolution. ZooM-CiTTY CO reconstructions are also shown for different values of  $D_z$ . The reconstructions are not exactly the same as those of Pissu *et al.* [2009] because of chemical loss of CO (25 ppbv in 5 days), and the fact that simulation started on 18 July instead of 15 July. The main conclusions are nevertheless the same: with a  $D_z$  value of  $1 \text{ m}^2 \text{ s}^{-1}$  the reconstruction reproduces the FF plume at the right place, with reasonable average CO concentrations, and the strong gradients at the plume edge are also well reproduced. CO values in the plume are slightly underestimated, by about 40 ppbv. It can also be noted that the reconstruction produces features that are not present in the data outside the plume. Apart from these discrepancies, simulated CO in the FF plume is strongly improved when using ZooM-CiTTY instead of MOCAGE model with both resolution. Measured and reconstructed  $O_3$  are shown in Figure 4. Simulated  $O_3$  concentrations are on average slightly lower than observed with larger differences at plume edges. These discrepancies are analyzed in more detail by comparing observations and simulation in  $O_3/\text{CO}$  space where air masses in the plume are characterized by high CO values.

#### 3.1.2. Trace Gas Correlations

[21] As well as a tool to easily distinguish between different air masses, species/CO correlations can be used to evaluate the main chemical characteristics in a model. Indeed a model may reproduce the main chemical characteristic of air masses

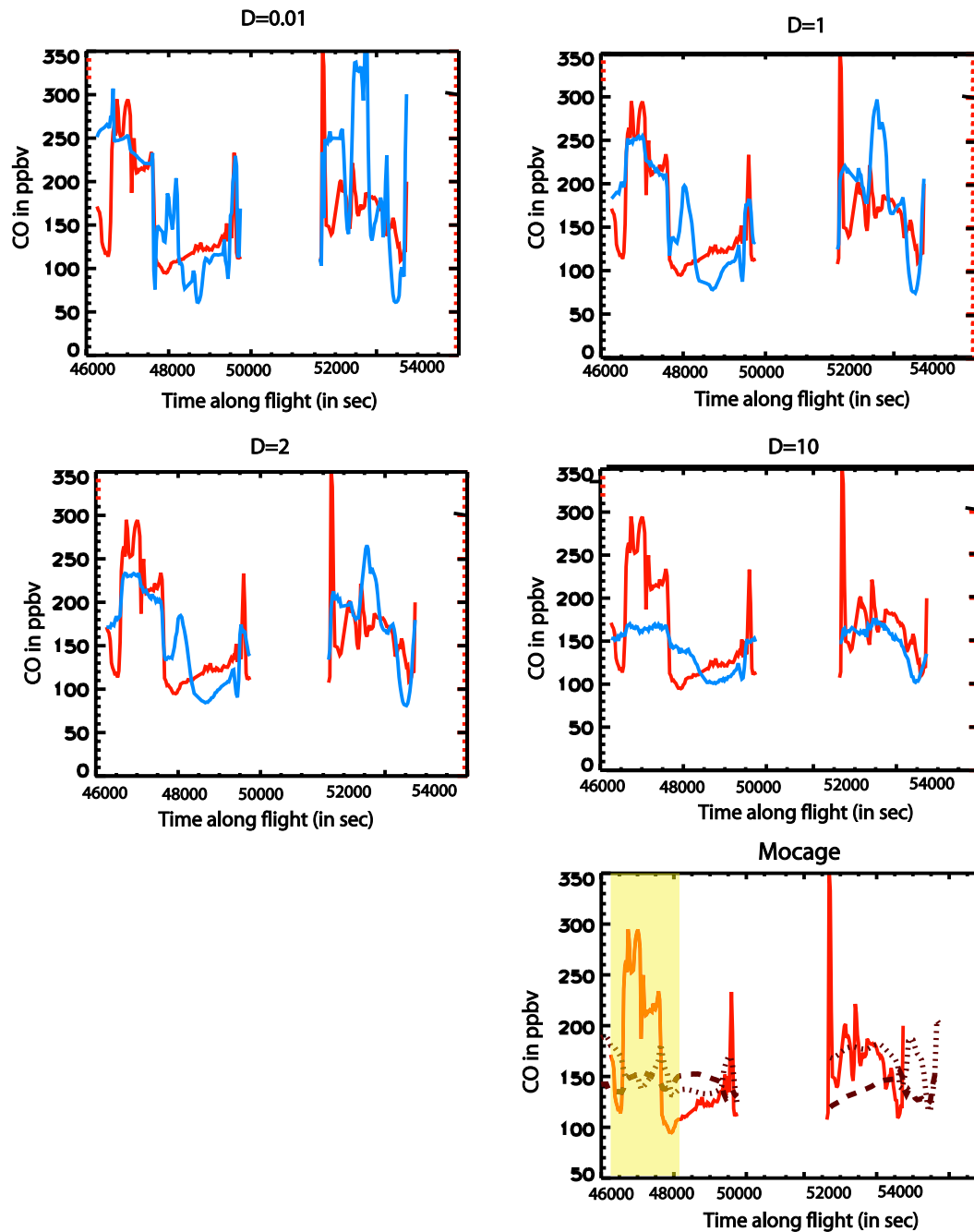


**Figure 3.** CO measured (red lines), simulated by MOCAGE (black dashed and dotted lines for  $2 \times 2$  and  $0.5 \times 0.5$  degree resolution, respectively), and simulated by Zoom-CiTTY (blue lines) for different values of the vertical turbulent diffusion  $D_z$  along two parts of the 23 July 2004 Falcon flight. Only the part highlighted in yellow in the Mocage plot was reconstructed with Zoom-CiTTY.

in a region but not exactly at the place where they were observed or with the right amplitude. A simple point by point comparison between model results and measurements along flight tracks would in this case show bad agreement whereas in species/CO space, an air mass is defined by its CO concentration and not its location.

[22] The FF plume is characterized by CO concentrations higher than 180 ppbv (also used in Figure 5 of *Real et al.* [2007]). The same limit is applied here whereas air masses with CO lower than 120 ppbv are considered to be outside

of the plume, and CO between 120 and 180 ppbv, at the edge of the plume.

[23] Measured and modeled Zoom-CiTTY  $O_3$  versus CO are shown in Figure 5. As previously noted,  $O_3$  and CO concentrations in the plume were underestimated by Zoom-CiTTY. However, it can be seen that reconstructed concentrations lie on the same  $O_3$ /CO slope as the observations. The observations give a slope of 7.6% compared to 6.5% from Zoom-CiTTY and 5.7% from *Real et al.* [2007]. In other words, even if CO and  $O_3$  are underestimated, the quantity of

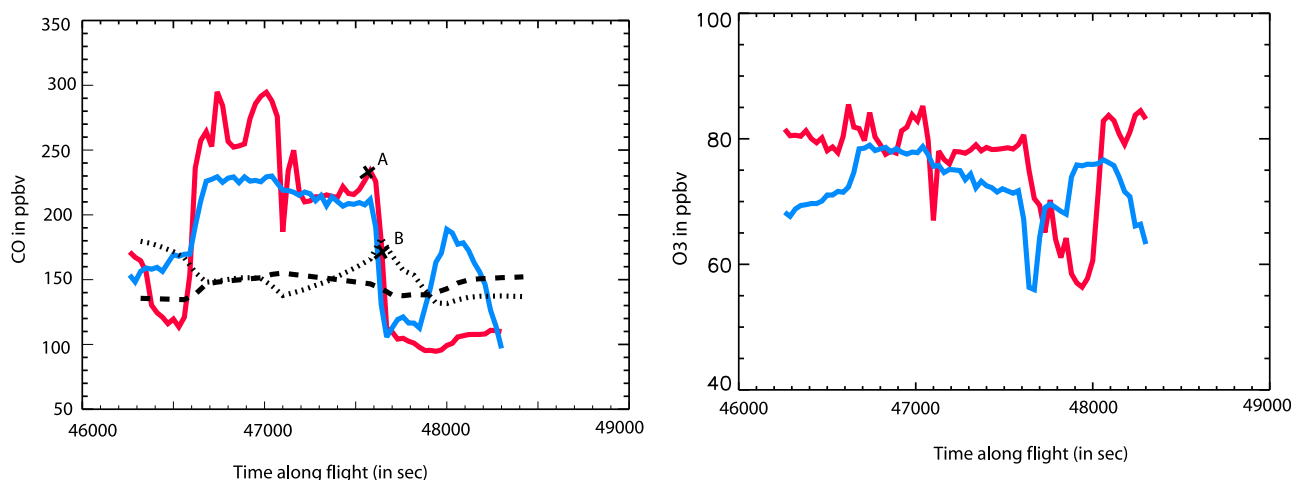


**Figure 4.** (left) CO and (right) O<sub>3</sub> measured (red lines) and simulated by ZooM-CiTty (blue lines) for the first FF plume sampled by the Falcon on 23 July 2004. MOCAGE CO values with  $2 \times 2$  and  $0.5 \times 0.5$  degree resolution are also represented as dashed and dotted black lines, respectively.

O<sub>3</sub> simulated per unit CO is generally correct. On the other hand, O<sub>3</sub> concentrations at the edge of the plume are underestimated as well as outside the plume (low CO). This underestimation may be caused by a transport of O<sub>3</sub> from the upper troposphere (UT) that was not very well captured in MOCAGE, or by nonresolved O<sub>3</sub> in situ production, by lightning for example.

[24] Results of ZooM-CiTty reconstructions with no chemistry simulated along the trajectories are also represented as pink stars in Figure 5. The main differences are found in the plume, where a negative O<sub>3</sub>/CO slope is simulated without chemistry. As explained by *Real et al.* [2007], the change from negative O<sub>3</sub>/CO slope observed in the plume on 18 July to positive slope on 23 July is due to O<sub>3</sub> production during transport from PAN decomposition.

[25] Observed and simulated NO<sub>y</sub>/CO correlations are also represented in Figure 5. In general, measurements and simulation are in close agreement except for high CO (and NO<sub>y</sub>) values that are not reproduced by the model. The measured

and simulated NO<sub>y</sub>/CO slopes agree remarkably well with values of 7 and 8%, respectively (pptv/ppbv). As ZooM-CiTty is initialized with global model fields scaled to the measurements in the FF plume and little or no NO<sub>y</sub> loss by deposition occurs in this case, these results are not so surprising but confirm the generally realistic simulation of air masses inside, outside and at the edge of the plume.

### 3.1.3. Net O<sub>3</sub> Production

[26] In this section, the mean net O<sub>3</sub> production simulated by ZooM-CiTty in the plume is compared with that simulated by *Real et al.* [2007]. Simulated mean (along the trajectories) O<sub>3</sub> destruction, production and net production are shown in Figure 6. Mean net simulated O<sub>3</sub> production in the plume (CO > 180 ppbv) is 1.8 ppbv/d, which is less than the 4 ppbv/d simulated in the study of *Real et al.* [2007]. Net O<sub>3</sub> production is also shown with respect to CO in Figure 6. There is a linear relation between these quantities in the FF plume. If the line is extrapolated to higher CO, the net O<sub>3</sub> production value corresponding to the CO mean value mea-

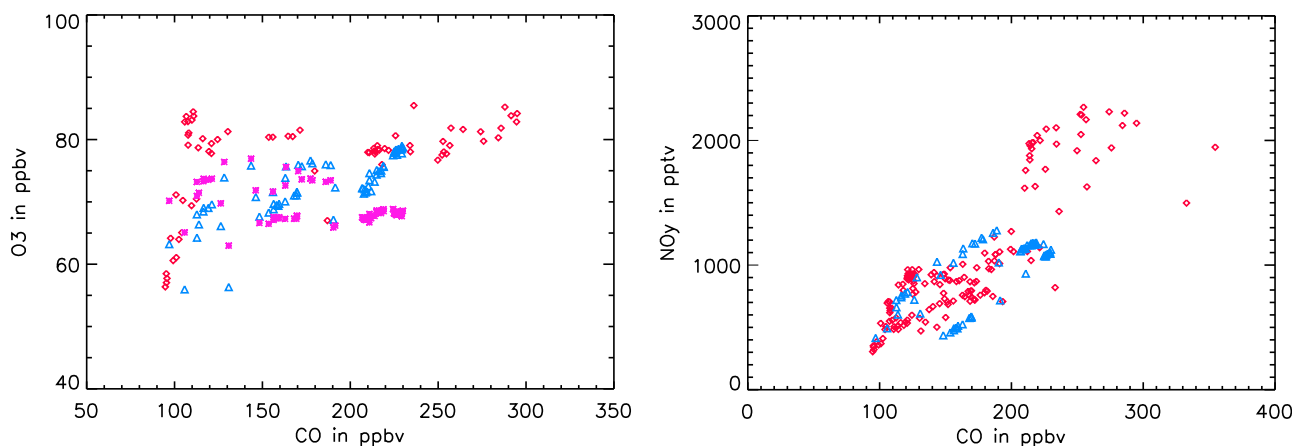


**Figure 5.** (left) O<sub>3</sub>/CO and (right) NO<sub>y</sub>/CO correlations measured (red diamonds) and simulated by ZooM-CiTty (blue triangles) for the plume on 23 July 2004. ZooM-CiTty O<sub>3</sub>/CO correlations without chemistry are also represented as pink stars in Figure 5 (left).

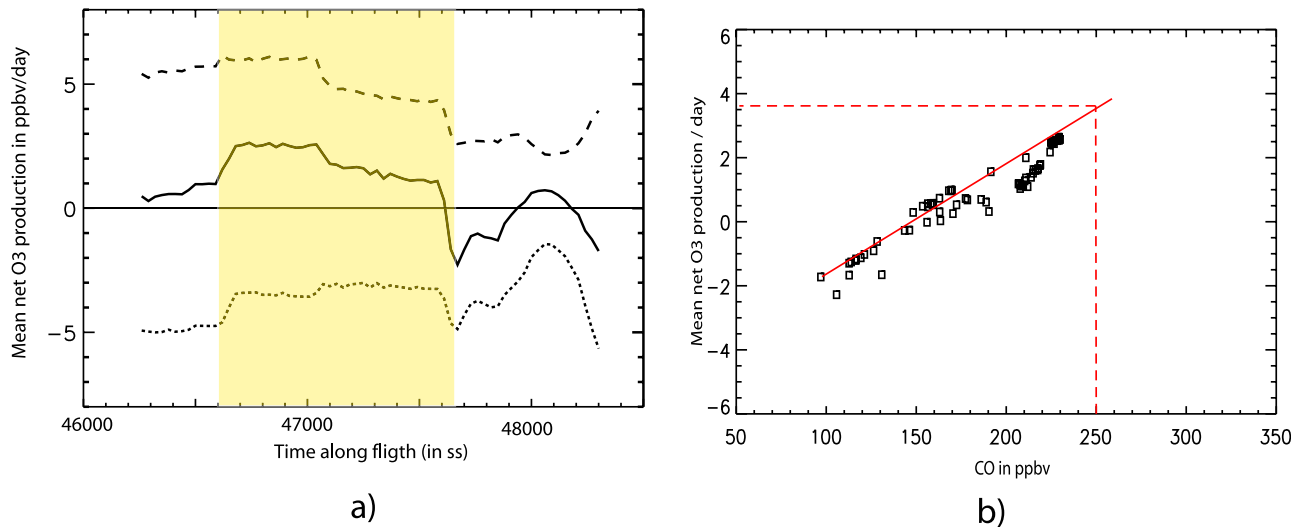


**Figure 6.** Daily O<sub>3</sub> production terms (averaged along trajectories) simulated on 23 July 2004. (a) Mean O<sub>3</sub> production (dashed line), destruction (dotted line), and mean net O<sub>3</sub> production (solid line) in ppbv per day. The FF plume is highlighted in yellow. (b) Mean net O<sub>3</sub> production versus CO concentrations.

sured in the plume (250 ppbv) is 3.75 ppbv/d, closer to the value of *Real et al.* [2007] which represents plume center conditions. These results suggest that O<sub>3</sub> production in ZooM-CiTTY is reasonable. At the same time, it helps to understand why the simple mixing method used by *Real et al.* [2007] was valid. Indeed, *Pisso et al.* [2009] showed that particles in the center of the FF plume were kept within the plume by the synoptic winds and so the hypothesis of homogeneous mixing in the plume was realistic in this case. This is discussed further in section 4. However, simple mixing parametrization as in the work by *Real et al.* [2007] cannot reproduce values at the edge of the plume where mixing is expected to be less homogeneous than inside the plume, as will be seen in section 3.2.

### 3.2. The 22 July DLR Falcon Flight Reconstruction

[27] It was shown that 23 July ZooM-Citty reconstruction was not able to represent the entire variability observed in the FF plume because pollutant levels were slightly underestimated, even if chemical production was well simulated. On this day, global models such as MOCAGE and TOMCAT [see *Cook et al.*, 2007] were not able to simulate clear CO enhancements at this location, and therefore ZooM-CiTTY results represent a significant improvement compared to these global models. The FF plumes observed by the DLR Falcon on 22 July over Spain were reproduced better by MOCAGE (see Figure 7) even if the plume was still smeared out compared to the data. The analysis of ZooM-CiTTY reconstructions on this day is thus particularly interesting. The 22 July

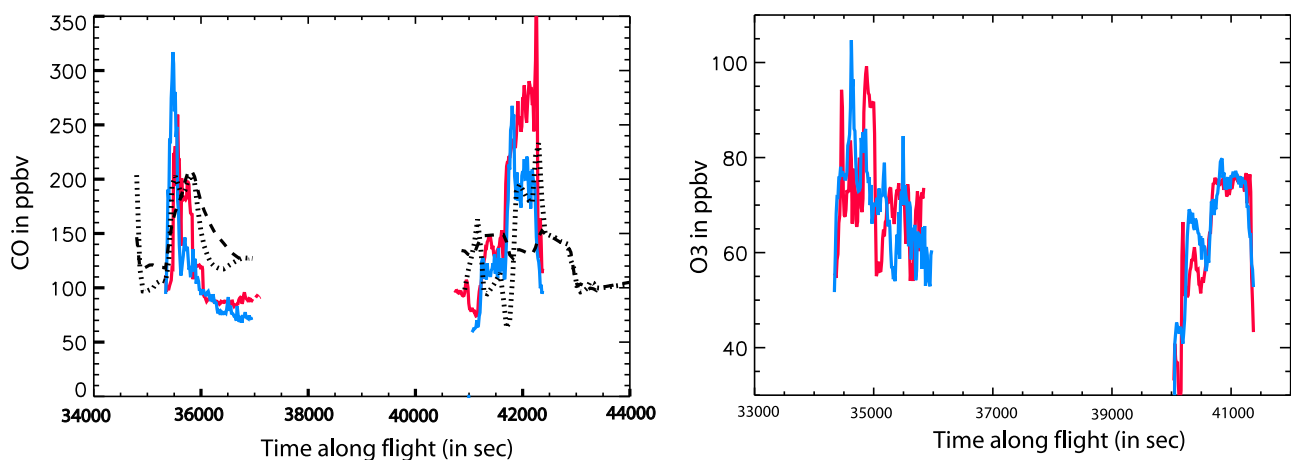


**Figure 7.** (left) CO and (right) O<sub>3</sub> measured (red lines) and simulated by ZooM-CiTTY (blue lines) on 22 July 2004. MOCAGE CO values with 2 × 2 and 0.5 × 0.5 degree resolution are also represented as dashed and dotted black lines, respectively.



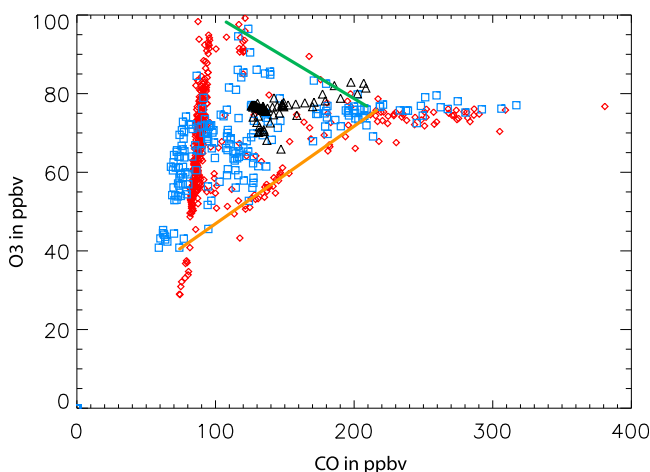


**Figure 8.**  $O_3/CO$  correlations on 22 July 2004, measured (red diamonds) and simulated by MOCAGE (black triangles) and ZooM-CiTTY (blue rectangles). Orange and green lines represent the so-called “mixing lines” (see section 3.2.2).

ZooM-CiTTY reconstruction used a value of  $D_z$  of  $1 \text{ m}^2 \text{ s}^{-1}$  [Pisso *et al.*, 2009]. Only two parts of the flight are shown, where FF plumes were encountered.

### 3.2.1. Temporal Series Comparison

[28] Measured and simulated CO (ZooM-CiTTY and MOCAGE with both resolution) and  $O_3$  (ZooM-CiTTY) concentrations along the flight are shown in Figure 7. As previously noted, MOCAGE with a 2 degree horizontal degree resolution tends to smear out CO concentrations downwind from sources leading to overestimated background concentrations and too weak concentration peaks, even if the modeled concentrations in the first observed plume are relatively well simulated (see Figure 7). Peaks are better simulated with a 0.5 horizontal degree resolution, especially the second one, but still smear out.

[29] Concerning ZooM-CiTTY simulations, the first CO peak is simulated earlier and maximum values are overestimated by about 50 ppbv. The second peak localization is well simulated but CO concentrations are underestimated by about 60 ppbv. The second peak CO value was already slightly underestimated in the reconstruction by Pisso *et al.* [2009] and is accentuated by the chemical CO loss in the ZooM-CiTTY runs. Compared to MOCAGE results with 0.5 horizontal degree resolution, the first peak is better simulated but it does not represent a strong improvement for the second peak. Concerning  $O_3$  values, the large variability observed in the first part of the flight and the relative homogeneity of measured  $O_3$  in the second part are well simulated. The ability of the model to reproduce  $O_3$  and net  $O_3$  production is better analyzed in  $O_3/CO$  space.

### 3.2.2. Trace Gas Correlations

[30] Measurements and model results from MOCAGE (original  $2^\circ$  resolution values interpolated along the flight track) and ZooM-CiTTY are represented in  $O_3/CO$  space in Figure 8. Whereas MOCAGE (black triangles) are too homogeneous, ZooM-CiTTY results are more representative of observed variability. Simulated values in FF plumes ( $CO > 180$  ppbv) are in good agreement with the measurements and the model is able to represent characteristic  $O_3$  and CO

relationships both inside and outside the plume. In particular, it reproduces the air masses with high  $O_3$  and low CO observed just above the plume which originate from the UTLS. Notice that these are mixed out in the global model simulations. ZooM-CiTTY simulates lower background CO concentrations (around 70 ppbv) than were observed (90 ppbv) pointing to differences in the initial fields. In the FF plumes,  $O_3/CO$  measured slopes are 3.5%, similar to those simulated by ZooM-CiTTY (2%), whereas MOCAGE slopes are too steep (12%).

[31] Not only  $O_3$  concentration is well reproduced by ZooM-CiTTY but also  $NO_y$ . Figure 9 shows ZooM-CiTTY simulation in the  $NO_y/CO$  space and show very good agreement between measured and simulated concentrations.

[32] One remarkable feature is the ability of ZooM-CiTTY to reproduce values observed at the plume edges that can be seen as mixing lines (orange and green) in Figure 8, i.e., lines that result from mixing two different air masses: FF and UT (Upper Troposphere) air masses (high  $O_3$  concentrations) for the green line, and FF with relatively clean air masses for orange line. In order to determine if such lines are due to mixing or chemical processing, reconstructions without chemistry were carried out and compared with ZooM-CiTTY (Figure 10, left). In the plume, the  $O_3/CO$  slope without chemistry is negative as was also observed 4 days before on 18 July. At the edge of the plume, the green line is reproduced almost identically by the nonchemistry reconstruction. The form of this line is thus mainly determined by mixing between FF and UT air masses and chemistry played a minor role. In contrast, the orange mixing line is not reproduced by nonchemistry reconstruction. In particular, runs without chemistry do not reproduce the observed low-CO, low- $O_3$  air masses. They do reproduce mixing between FF and air masses with low CO but these low-CO air masses have higher simulated  $O_3$  concentrations than measured. In Figure 10 (right), ZooM-CiTTY reconstruction points are colored with their initial water vapor levels (in g/kg) and the low-CO air masses show high initial water vapor content (PBL origin). Therefore, high  $O_3$  chemical destruction due to high water vapor can explain the low observed final  $O_3$  that is not reproduced in runs without chemistry.

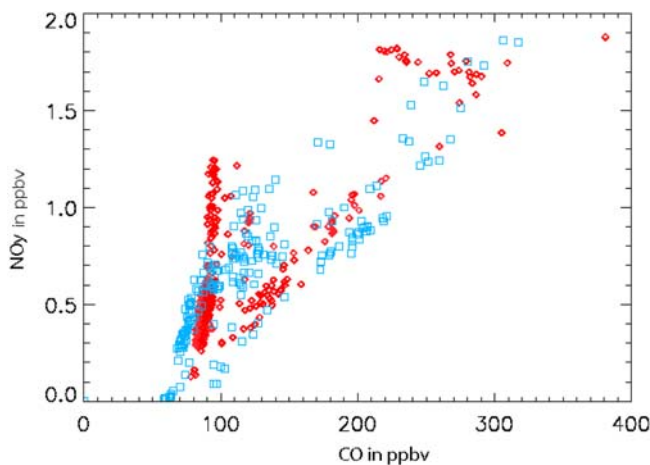


**Figure 9.**  $NO_y$  concentrations measured (red) and simulated (blue) by ZooM-CiTTY on the 22 July 2004 Falcon flight.

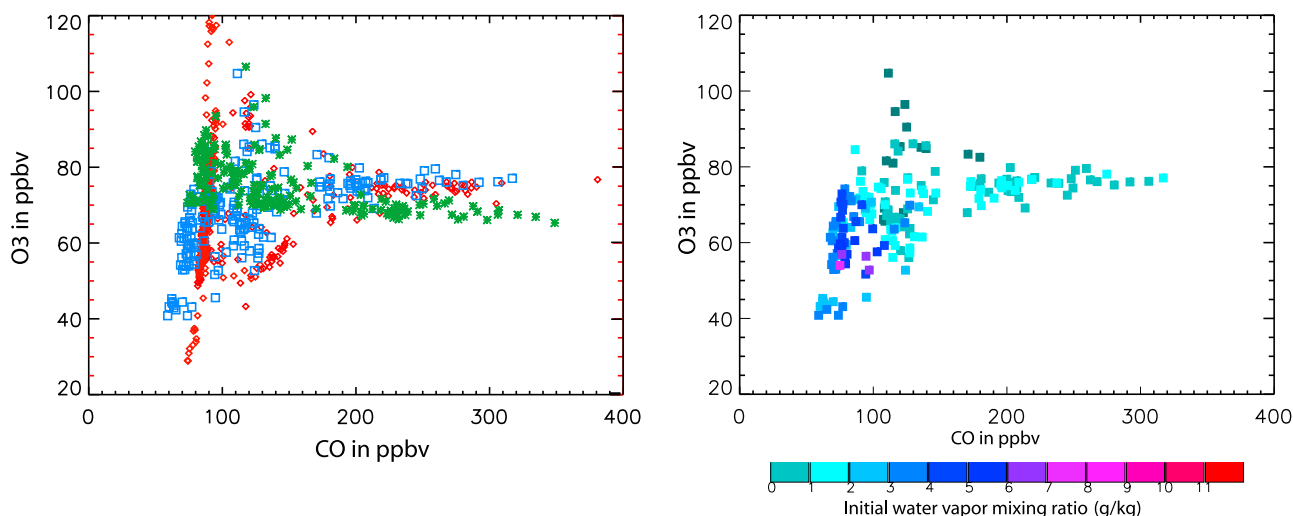


**Figure 10.** (left)  $O_3/CO$  correlations on 22 July 2004, measured (red diamonds), simulated by ZooM-CiTTY (blue rectangles), and reconstructed with no chemistry (green stars). (right) ZooM-CiTTY  $O_3/CO$  colored by initial simulated water vapor content (in g/kg).

[33] Global models do not currently have the required resolution to represent such mixing lines (see Figure 8), and a classical Lagrangian reconstruction would also badly represent them because it would simulate too much variation of composition between isolated air masses. ZooM-CiTTY is able to reproduce these features because it represents the composition of an air parcel as the contribution of several air masses with different origins and simulates chemical evolution of all these air masses. Observed  $O_3/CO$  mixing lines have been used previously to characterize mixing of air masses in the lower stratosphere [Ray *et al.*, 2004] or mixing in frontal zones [Esler *et al.*, 2003]. Mixing lines between HCl and  $O_3$ , have also been used to evaluate the fraction of stratospheric air entering the troposphere [Marcy *et al.*, 2004]. However, these analysis are dependent on the estimation of background concentrations (for mixing) and do not take into account chemical processes. The ability of the ZooM-CiTTY simulations to reproduce mixing lines may for example, allow the processes which govern the formation of such lines to be determined in such cases.

[34]  $O_3/CO$  correlations are also often used to estimate  $O_3$  production in plumes with high  $O_3/CO$  correlations associated with high  $O_3$  production. Several studies [Goode *et al.*, 2000; Andreae *et al.*, 1988; Duck *et al.*, 2007] related different observed values of  $O_3/CO$  slopes (from 4% to 80%) supposing very different  $O_3$  production in plumes. Other studies also relied on comparison between  $O_3/CO$  slopes simulated by global models and measured (averaged over model grid boxes) to validate modeled  $O_3$  production [Pfister *et al.*, 2006]. The analysis performed here using ZooM-CiTTY correlations shows that the use of correlation slopes must be performed carefully. For example, between 120 and 180 ppbv for CO, a strong positive slope (orange line) is the result of mixing and chemical  $O_3$  destruction rather than  $O_3$  production, and a strong negative slope (green line) is the result of mixing alone and not  $O_3$  destruction. Only in the center of the plume, where mixing is slow and uniform, is the  $O_3/CO$  slope mainly due to chemistry. Therefore, the limits

used to select air masses that are considered to be in pollutant plumes are crucial.

#### 4. Influence of Chemical Nonlinearity on ZooM-CiTTY Simulations

[35] In the method used up to now, the concentrations of the  $N$  air masses contributing to final concentrations of the same point are only mixed at the end. Thus, there is no mixing between these parcels during transport. In the real atmosphere, it is likely that the  $N$  air masses, or at least a subset, do interact with each other during their transport. This mixing may have an influence on final concentrations because of the nonlinearity of tropospheric chemistry. In order to explore this point, a sensitivity test was conducted. Instead of averaging air mass concentrations at the end of the runs, the simulation was stopped after a time  $\delta T_{mix}$  and parcel positions stored. Parcels that were closer than a horizontal distance of  $\delta l_{mix}$  and a vertical distance of  $\delta z_{mix}$  were mixed, i.e., their concentrations averaged and reattributed to all mixed particles within the space  $\delta z_{mix} \times \delta T_{mix}$ . The goal of this test was to evaluate if on-route mixing could have had a strong impact on simulated concentrations, and therefore a large  $\delta l_{mix}$  was chosen.

[36] Figure 11 shows CO and  $O_3$  concentrations modeled for the first CO peak observed by the Falcon on 22 July. Concentrations simulated with mixing at the end of the simulation are in black. Green lines represent simulations with a  $\delta T_{mix}$  of 2 days (half the simulation time),  $\delta l_{mix}$  of 180 km and  $\delta z_{mix}$  of 50 m. This is equivalent to MOCAGE horizontal resolution but with higher vertical resolution. Both CO and  $O_3$  concentrations are similar with and without mixing after 2 days. The only small difference is seen in the center of the plume where  $O_3$  concentrations with mixing are lower by about 2 ppbv. This leads to enhanced CO concentration (5 ppbv) due to lower OH production.

[37] These small differences can be explained in terms of parcel separation which is different within the plume and at its

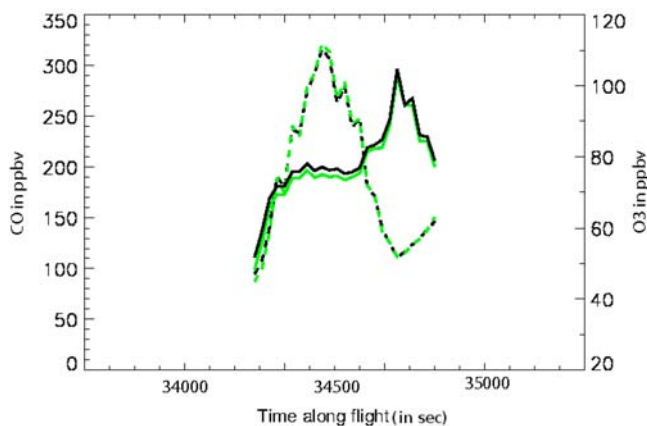


**Figure 11.** Modeled CO (dashed lines) and O<sub>3</sub> (solid lines) concentrations with (green line) and without (black line) mixing after 2 days, for the first plume encountered by the Falcon on 22 July 2004.

edges in this particular case of long-range transport. As explained by *Pisso et al.* [2009], synoptic winds kept parcels together in the plume whereas at the edges, parcels are more dispersed and have chemical characteristics that can be very different. This feature can be visualized in Figure 12 which shows the initial positions of 500 parcels initialized at a point located in the plume (point A in Figure 4), and at the plume edge (point B in Figure 4). Each parcel is colored with CO interpolated from MOCAGE. Figure 12 clearly shows that with the same value of  $D_z$ , the dispersion of parcels is different inside and outside of the plume. Therefore, air masses located at the edge of the plume rapidly separated by more than 2 degrees, and are no longer mixed in the mixing procedure used here. In contrast, air masses in the plume stay closely grouped and are more subject to the mixing procedure but the effect is small since the air masses have very similar chemical composition.

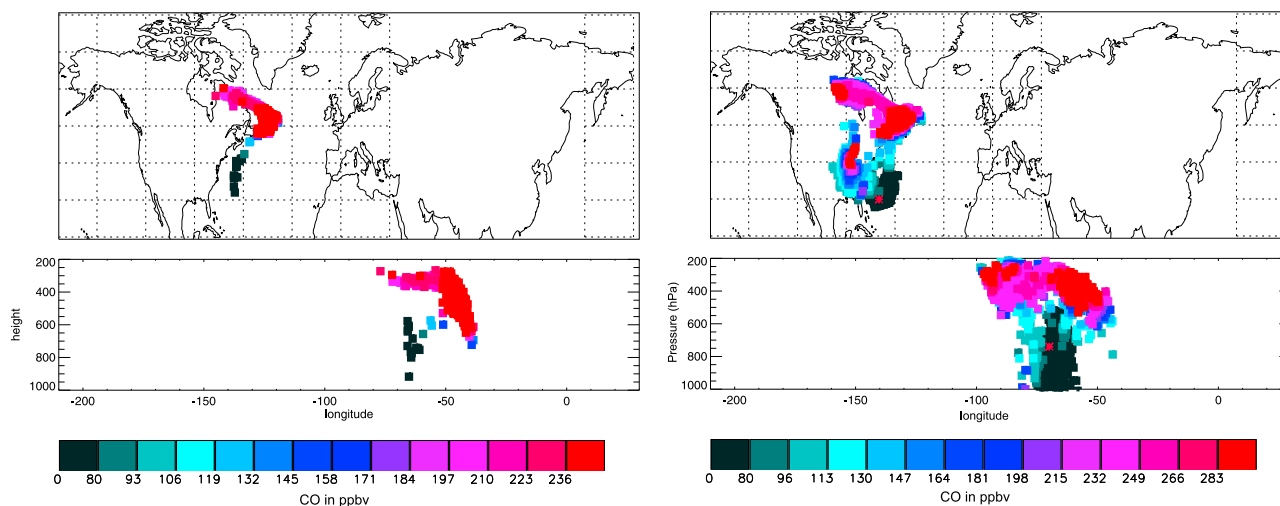


**Figure 12.** Initial positions (5 days before) of the 2000 particles initialized at (left) point A and (right) point B along the Falcon flight (see Figure 4). Each particle is colored by MOCAGE CO values interpolated in time and location.

[38] To summarize, air masses at the edges of plumes have distinct origins and thus more ‘potential’ to induce changes in concentration, but they also separate very rapidly and in the real atmosphere will probably not interact for a long time, whereas air masses in the plume are more likely to interact but present less variability in their concentrations. It is because ZooM-CiTTY treats advection of parcels separately that the online mixing procedure does not lead to strong differences in concentrations. In a Eulerian model, this parcel advection is not performed and mixing in coarse model grids can lead to errors in calculated reaction rates. This is studied in section 5.

[39] It was shown that errors due to mixing procedure are not important in cases where gradients are maintained by large-scale winds. This ZooM-CiTTY method is thus adapted for studying strong layering structures in the troposphere. However to apply such a modeling in broader cases, interaction between parcels “en route” must be taken into account.

## 5. Estimation of Grid Resolution Errors in Net O<sub>3</sub> Production Rates

[40] ZooM-CiTTY was successfully evaluated for two cases (section 3) and a sensitivity test suggests that the adopted mixing procedure does not induce important errors in this case. ZooM-CiTTY represents results from a high-resolution model and as such can be used to evaluate possible errors associated with averaging concentrations over larger regions representative of global model grids. On 22 July, 100 particles were released every 15 s, which represents approximately 100 particles every 2.5 km. Since O<sub>3</sub> chemistry is nonlinear, different O<sub>3</sub> production rates can be simulated by models with different resolution. This effect has been examined previously [*Crowther et al.*, 2002; *Esler et al.*, 2004] by averaging observations and calculating O<sub>3</sub> production over different temporal and spatial scales. Here, we make use of the ZooM-CiTTY results as the reference simulation. The hourly instantaneous ZooM-CiTTY net O<sub>3</sub> production rates at the end of the 100 simulations per point along

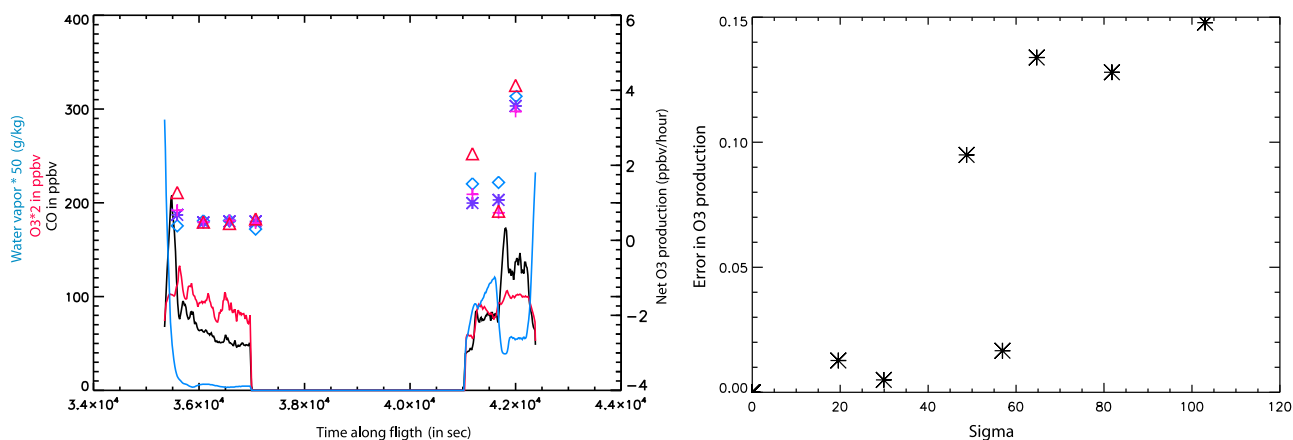


**Figure 13.** (left) ZooM-CiTTY CO, O<sub>3</sub>, and water vapor (in g/kg × 100) along the 22 July 2004 flight (black, red, and blue lines, respectively) and averaged O<sub>3</sub> net production (see text) in the simulation with 100 km box (blue diamonds), 50 km box (violet stars), 25 km box (pink crosses), 2.5 km box (red triangles), and ZooM-CiTTY net production (red rectangles). (right) Differences in net O<sub>3</sub> production between the 100 km (1°) box simulation and ZooM-CiTTY (in ppbv/h) versus ZooM-CiTTY CO variance ( $\sigma_{\text{CO}}$ ) + O<sub>3</sub> variance ( $\sigma_{\text{O}_3}$ ) in the 100 km box (Sigma).

the flight track are averaged. These results can be compared with hourly instantaneous production rates calculated using mean O<sub>3</sub> precursors concentrations of the 100 parcels representing averages over 2.5 km.

[41] They can also be compared with averages calculated by averaging concentrations over larger spatial scales. In practice, concentrations simulated with ZooM-CiTTY were averaged every 150, 300 and 600 s which represent grids of approximately 25, 50 and 100 km, or about 0.25, 0.5 and 1 degree. Hourly instantaneous O<sub>3</sub> net production rates were calculated from these averaged concentrations using the box model (CiTTYCAT). Finally, these net O<sub>3</sub> production rates for grids of 2.5, 25 and 50 km and from the original ZooM-CiTTY simulations were averaged over 100 km (1°) boxes in order to be compared. Results are shown in Figure 13 (left) together with ZooM-CiTTY CO, O<sub>3</sub> and water vapor. The differences between ZooM-CiTTY net O<sub>3</sub> production rates and the rates calculated using mean concentrations at the same resolution (2.5 km) are larger at the edges of the plumes where the N air masses exhibit the largest range of concentrations but they do not exceed 5–10%. In contrast, the percentage difference between O<sub>3</sub> net production simulated with ZooM-CiTTY and averaging over a 1° grid, varies between 0 and more than 50%, representing about 7 ppbv differences over the 5 day run. If this difference is represented as a function of the sum of the CO plus O<sub>3</sub> variances simulated by ZooM-CiTTY in the 1° box (Figure 13, right), it can be seen that strong variances are associated with strong differences in net O<sub>3</sub> production. In other words, when strong gradients or strong inhomogeneity are present in a box, nonlinearity becomes important. In this case, the largest differences are found at the edges of the plume. In ZooM-CiTTY, gradients at these edges are conserved by the large-scale winds and air masses inside and outside the plume do not interact with each other whereas in the 1° results these gradients are smeared out and air masses mixed. Since these air masses have strong differences in chemical composition, this leads to large differences in average net O<sub>3</sub> production.

[42] Depending on the case, O<sub>3</sub> production can be underestimated or overestimated compared to ZooM-CiTTY and depends on the correlation between averaged species at different resolutions. Indeed, as shown by *Crowther et al.* [2002], if reactants are correlated, a coarser resolution will underestimate the products whereas if they are anticorrelated the products will be overestimated. For O<sub>3</sub>, both photochemical production and destruction reactions need to be analyzed.

[43] In boxes B, C and D (outside the FF plume) concentration gradients are low and net production from ZooM-CiTTY and the 1° box simulation are similar. In boxes A and F (plume edges), O<sub>3</sub> production and destruction (not shown) are overestimated by the 1° simulation. In the low-resolution case, air masses with low O<sub>3</sub> and high water vapor are present in the same grid as air masses with high O<sub>3</sub> and low water vapor. Therefore, averaging will lead to overestimation of reactions involving O<sub>3</sub> and water vapor, which is the case for O<sub>3</sub> destruction (through O<sub>3</sub> photolysis) and O<sub>3</sub> production (through the formation of OH and HO<sub>2</sub> and reaction with NO). However in box A, O<sub>3</sub> production is overestimated more than O<sub>3</sub> destruction whereas the opposite is the case in box F. As a result, O<sub>3</sub> net production is underestimated in box A and overestimated in box F. In box E, water vapor and O<sub>3</sub> are correlated (BL air masses) leading to an underestimation in both O<sub>3</sub> production and destruction, and as production is more underestimated than destruction net O<sub>3</sub> production is also underestimated. Finally in box G (in the plume) where air masses are mainly FF in nature, with relatively low water vapor and correlated O<sub>3</sub>, NO<sub>x</sub> and VOC, the main difference is an underestimation of O<sub>3</sub> production, resulting in a net O<sub>3</sub> production underestimation of about 5%. Overall, differences in net O<sub>3</sub> production are low in the FF plumes (5%) and strong at their edges (between 20 and 50%).

[44] This analysis can be compared to results from *Esler et al.* [2004] and *Crowther et al.* [2002]. They degraded the resolution of measurements taken during aircraft campaign in

the UTLS region to calculate OH and O<sub>3</sub> production rates at different spatial resolutions. They evaluated that on average OH production is overestimated by 5–20% but can reach 50% in some cases, and net O<sub>3</sub> production is also overestimated by 5–10% on average in the northern midlatitude UTLS. *Wild and Prather* [2006] also quantified errors due to grid resolution by comparing global model results over Asia with resolution ranging from 5.5° to 1.1°. They evaluated a linear evolution of errors due to grid resolution from 27% to 5% at 1.1° resolution close to continental emissions and negligible errors in the free troposphere at 1.1° resolution. The results of our study cannot be directly compared with *Wild and Prather* [2006] because a simple case study is not representative of a more general region of the atmosphere; Nevertheless, our results suggest that in particular cases, where strong gradients in O<sub>3</sub> precursors are maintained, the errors can be as large as 50%. In addition, errors can be nonlinear such as in boxes E and F where errors are more important at 0.25° and 0.50° than at 1°. Other results [*Esler et al.*, 2004] also suggest that errors due to grid resolution may be nonlinear at resolutions below 1°. According to *Newell et al.* [1996], 20% of the troposphere is occupied by distinct layers, defined by gradients between air masses. Further analysis is required to determine the importance of errors in net O<sub>3</sub> production of 20 to 50% at plume edges which may certainly be important locally. Global models are currently not run at resolutions sufficient to reproduce observed gradients between air masses. The results of *Pisso et al.* [2009] based on the simulation of CO tracer suggested that horizontal resolutions of at least 40 km are required to reproduce the dynamical structure of pollutant plumes in the free troposphere. As errors in O<sub>3</sub> production up to 50% are simulated for a resolution of 25 km, results presented here suggest that higher resolutions maybe required in order to correctly reproduce chemical evolution of plumes during long-range transport.

## 6. Conclusions

[45] In this paper, we present a new modeling approach, ZooM-CiTty for the reproduction of observed layering structures on pollutants in the free troposphere. Photochemical simulations were coupled to the ensemble parcel model of *Pisso et al.* [2009] which includes a stochastic representation of mixing, in order to perform high resolution reconstructions of aircraft measurements. The model was used to examine the evolution of reactive chemical species, and in particular O<sub>3</sub>, in the same case studied by *Pisso et al.* [2009]. In this case, the DLR Falcon made interceptions of a forest fire plume observed several days previously by the NASA DC8 as part of the Lagrangian 2K4 ICARTT experiment in summer 2004. Ensembles of back trajectories, released every 15 s or 30s along flights, were initialized using coarse resolution global model (MOCAGE) chemical fields (2° × 2° and 0.5° × 0.5°) forced toward measurements in the FF plume. Model results were compared to measured O<sub>3</sub>, CO and NO<sub>y</sub> during two flights of the DLR Falcon over Europe. Averages of all parcels arriving at each measurement point were compared to observed concentrations. The errors due to the mixing-but-no-interaction procedure (no mixing during the transport) in the model were also evaluated. It appears that as long as the gradients are driven by synoptic winds this error is not too significant, at least with back trajectories not older than

6 days. Therefore this method is appropriate to study layering structures in the free troposphere.

[46] ZooM-CiTty produces high-resolution results which generally reproduce well observed levels of trace gases both inside the plumes and at the edges of the FF plumes compared to the global model results. Discrepancies between the model results and the measurements can be attributed to errors in trajectory position or errors in the initial model fields.

[47] This modeling approach also shows that each measurement is an average of different air mass origins. As such it can be used to examine the processes which contribute to observed trace gas correlations. Indeed one very interesting feature of the model is its capability to reproduce observed mixing lines between different air masses in O<sub>3</sub>/CO space. In the case of the flight on the 22 July 2004, the model was used to discriminate in the observed O<sub>3</sub>/CO correlation across the plume the part only due to mixing and the part due to photochemical O<sub>3</sub> destruction the model was used to show that part of the observed correlation across the plume was due only to mixing and part was due to photochemical O<sub>3</sub> destruction.

[48] The high-resolution ZooM-CiTty results, approximately representing 2.5 km horizontal resolution, were used to assess the importance of errors due to nonlinear tropospheric chemistry when averaging over a large domain, as in coarse resolution models. It was shown that in the case where strong concentration gradients are maintained by large-scale winds (at the plume edge in this case), errors in net O<sub>3</sub> production at coarser resolutions can be large (up to 50%) even at relatively small grid scales (25 km).

[49] To conclude, ZooM-CiTty can be seen as a magnifying glass, with the capacity to zoom over a very detailed part of the atmosphere, only using information contained in a much coarser global model. It produces results at very high resolution over a limited area and take into account long-range transport processes. It can be used to examine in detail the processes leading to observed layering structures on pollutant concentrations. Comparison with global model results allows quantification of errors in such models, in particular, those related to grid resolution.

[50] However to apply this model to broader cases a better representation of mixing is required. For example using the following formulation: one parcel is released for one measured point and is divided in 2 every time stretching become important (to be defined) along transport, leading, as previously, to a set of parcels representing at the end one measured point but taking into account mixing during transport.

[51] **Acknowledgments.** Elsa Real and Kathy Law acknowledge financial support from national programs (PNCA, PATOM) provided by INSU, ADEME, and also from Institut Pierre Simon Laplace (IPSL), as well as the Institut Geographique National (IGN) for hosting the DLR Falcon campaign at Creil, France. We would like to thank the whole ICARTT team and, in particular, DLR scientists. Ignacio Pisso was funded with a fellowship of Ecole Polytechnique.

## References

- Andreae, M. O., et al. (1988), Biomass-burning emissions and associated haze layers over Amazonia, *J. Geophys. Res.*, 93, 1509–1527.
- Arnold, S. R., et al. (2007), Quantification of mean OH concentration and air mass dilution rates from successive observations of non-methane hydrocarbons in single air masses, *J. Geophys. Res.*, 112, D10S40, doi:10.1029/2006JD007594.

- Bousserez, N., et al. (2007), Evaluation of MOCAGE CTM during the ICARTT/ITOP experiment, *J. Geophys. Res.*, *112*, D10S42, doi:10.1029/2006JD007595.
- Cook, P., et al. (2007), Forest fire plumes over the North Atlantic: p-TOMCAT model simulations with aircraft and satellite measurement from the ITOP/ICARTT campaign, *J. Geophys. Res.*, *112*, D10S43, doi:10.1029/2006JD007563.
- Crowther, R. A., K. S. Law, J. A. Pyle, S. Bekki, and H. G. J. Smit (2002), Characterising the effect of large-scale model resolution upon calculated OH production using MOZIC data, *Geophys. Res. Lett.*, *29*(12), 1613, doi:10.1029/2002GL014660.
- Duck, T. J., et al. (2007), Transport of forest fire emissions from Alaska to Nova Scotia during summer 2004, *J. Geophys. Res.*, *112*, D10S44, doi:10.1029/2006JD007716.
- Eslser, J. G., D. G. H. Tan, P. H. Haynes, M. J. Evans, K. S. Law, P.-H. Plantevin, and J. A. Pyle (2001), Stratosphere-troposphere exchange: Chemical sensitivity to mixing, *J. Geophys. Res.*, *106*, 4717–4732.
- Eslser, J. G., P. H. Haynes, K. S. Law, H. Barjat, K. Dewey, J. Kent, S. Schmitgen, and N. Brough (2003), Transport and mixing between air-masses in cold frontal regions during Dynamics and Chemistry of Frontal Zones, *J. Geophys. Res.*, *108*(D4), 4142, doi:10.1029/2001JD001494.
- Eslser, J. G., G. J. Roelofs, M. O. Khler, and F. M. O'Connor (2004), A quantitative analysis of grid-related systematic errors in oxidising capacity and ozone production rates in chemistry transport models, *Atmos. Chem. Phys.*, *4*, 1781–1795.
- Evans, M. J., et al. (2000), Evaluation of a Lagrangian box model using field measurements from EASE (Eastern Atlantic Summer Experiment) 1996, *Atmos. Environ.*, *34*, 3843–3863.
- Fehsenfeld, F., et al. (2006), International Consortium for Atmospheric Research on Transport and Transformation (ICARTT): North America to Europe—Overview of the 2004 summer field study, *J. Geophys. Res.*, *111*, D23S01, doi:10.1029/2006JD007829.
- Goode, J., R. J. Yokelson, D. E. Ward, R. E. Babbit, M. A. Davies, and W. M. Hao (2000), Measurements of excess O<sub>3</sub>, CO<sub>2</sub>, CH<sub>4</sub>, C<sub>2</sub>H<sub>2</sub>, HCN, NO, NH<sub>3</sub>, HCOOH, CH<sub>3</sub>COOH, HCHO, and CH<sub>3</sub>OH in 1997 Alaskan biomass burning plumes by airborne Fourier transform spectroscopy (AFTIR), *J. Geophys. Res.*, *105*, 22,147–22,166.
- Hough, A. (1988), The calculation of photolysis rates for use in global tropospheric modeling studies, technical report, Energy Res. Estab., Her Majesty's Stn. Off., London.
- Jacob, D. J., J. A. Logan, and R. M. Yevich (1993), Simulation of summertime ozone over North America, *J. Geophys. Res.*, *98*, 14,797–14,816.
- Lefevre, F., P. Simon, and G. P. Brasseur (1994), Chemistry of the 1991/1992 stratospheric winter: Three-dimensional model simulations, *J. Geophys. Res.*, *99*, 8183–8195.
- Legras, B., B. Joseph, and F. Lefevre (2003), Vertical diffusivity in the lower stratosphere from Lagrangian back-trajectory reconstructions of ozone profiles, *J. Geophys. Res.*, *108*(D18), 4562, doi:10.1029/2002JD003045.
- Marcy, T. P., et al. (2004), Quantifying stratospheric ozone in the upper troposphere with in situ measurements of HCl, *Science*, *304*, 261–265.
- Methven, J., and B. Hoskins (1999), The advection of high-resolution tracers by low-resolution winds, *J. Atmos. Sci.*, *56*, 3262–3285.
- Methven, J., S. R. Arnold, F. M. O'Connor, H. Barjat, K. Dewey, J. Kent, and N. Brough (2003), Estimating photochemically produced ozone throughout a domain using flight data and a Lagrangian model, *J. Geophys. Res.*, *108*(D9), 4271, doi:10.1029/2002JD002955.
- Methven, J., et al. (2006), Establishing Lagrangian connections between observations within air masses crossing the Atlantic during the ICARTT experiment, *J. Geophys. Res.*, *111*, D23S62, doi:10.1029/2006JD007540.
- Newell, R. E., Z. X. Zhu, W. Hu, E. V. Browell, G. L. Gregory, G. W. Sachse, J. E. Collins, K. K. Kelly, and S. C. Liu (1996), Vertical fine-scale atmospheric structure measured from NASA DC-8 during PEM-West A, *J. Geophys. Res.*, *101*, 1943–1960.
- Pfister, G. P., et al. (2006), Ozone production from the 2004 North American boreal fires, *J. Geophys. Res.*, *111*, D24S07, doi:10.1029/2006JD007695.
- Pisso, I., E. Real, K. S. Law, B. Legras, N. Bousserez, M. Attié, and H. Schlager (2009), Estimation of mixing in the troposphere from lagrangian trace gas reconstructions during long-range pollution plume transport, *J. Geophys. Res.*, *114*, D19301, doi:10.1029/2008JD011289.
- Pyle, J. A., and A. M. Zavody (1990), The modelling problems associated with spatial averaging, *Q. J. R. Meteorol. Soc.*, *116*, 753–766.
- Ray, E. A., et al. (2004), Evidence of the effect of summertime midlatitude convection on the subtropical lower stratosphere from CRYSTAL-FACE tracer measurements, *J. Geophys. Res.*, *109*, D18304, doi:10.1029/2004JD004655.
- Real, E., et al. (2007), Processes influencing ozone levels in Alaskan forest fires plumes during long-range transport over the North Atlantic, *J. Geophys. Res.*, *112*, D10S41, doi:10.1029/2006JD007576.
- Rolph, G., and R. Draxler (1990), Sensitivity of three-dimensional trajectories to the spatial and temporal densities of the wind field, *J. Appl. Meteorol.*, *29*, 1043–1054.
- Stockwell, W. R., F. Kirchner, and S. S. M. Kuhn (1997), A new mechanism for regional atmospheric chemistry modelling, *J. Geophys. Res.*, *102*, 25,847–25,879.
- Turquety, S., et al. (2007), Inventory of boreal fire emissions for North America in 2004: Importance of peat burning and pyro-convection injection, *J. Geophys. Res.*, *112*, D12S03, doi:10.1029/2006JD007281.
- Wild, O., and M. J. Prather (2006), Global tropospheric ozone modeling: Quantifying errors due to grid resolution, *J. Geophys. Res.*, *111*, D11305, doi:10.1029/2005JD006605.
- Wild, O., K. S. Law, D. S. McKenna, B. J. Bandy, S. A. Penkett, and J. A. Pyle (1996), Photochemical trajectory modeling studies of the North Atlantic region during August 1993, *J. Geophys. Res.*, *101*, 29,269–29,288.
- J. L. Attié, Laboratoire d'Aérodologie, CNRM, F-31000 Toulouse, France.
- N. Bousserez, Department of Physics and Atmospheric Science, Dalhousie University, Halifax, NS B3H 4H8, Canada.
- K. S. Law, LATMOS, Université Pierre et Marie Curie, CNRS, F-75005 Paris, France.
- B. Legras, Laboratoire de Météorologie Dynamique, IPSL, F-75005 Paris, France.
- I. Pisso, DAMTP, University of Cambridge, Cambridge, CB3 9DA, UK.
- E. Real, CERE, ENPC, EDF, Université Paris-Est, 20 rue Alfred Nobel, Champs sur Marne, F-77455 Marne le Vallée, France. (reale@cerea.enpc.fr)
- A. Roiger and H. Schlager, Deutsches Zentrum für Luft- und Raumfahrt, Institut für Physik der Atmosphäre, D-82234 Wessling, Germany.